A Flexible Appendage Model for Use in Integrated Control/Structure Spacecraft Design

J. Alvaro PEREZ [*] Christelle PITTET [**]
Daniel ALAZARD [***] Thomas LOQUEN [*]
Christelle CUMER [*]

[*] *ONERA System Control and Flight Mechanics Department, Toulouse, 31000 France (e-mail: Jose-Alvaro.Perez_Gonzalez@onera.fr; thomas.loquen@onera.fr; christelle.cumer@onera.fr).*
[**] *Centre National d'Etudes Spatiales (CNES), Toulouse, 31000 France (e-mail: christelle.pittet@cnes.fr)*
[***] *Institute Superieur de l'Aeronautique et de l'Espace, Toulouse, France, (e-mail: daniel.alazard@isae.fr)*

Abstract The study presents and validates a flexible appendage model to be used in an integrated control/structure spacecraft design. The integrated design methodology needs an accurate LFT representation of spacecraft flexible appendages so that parametric variations can be included. This requirement can be met using the Interconnected Flexible Appendage model studied in Perez et al. (2015). The model suitability is validated through the modeling of a real deployable boom, obtaining the same frequency modes and dynamical behavior.

Keywords: Integrated Design, Structured H_∞ Synthesis, Flexible Structures, Attitude Control System (ACS), Linear Fractional Representation (LFT).

1. INTRODUCTION

The design of new generation space vehicles is increasingly becoming subject to design integration, that is, close coordination in the design of various systems constitutive of the spacecraft. For example, space structures involving very large complex chains composed by rigid and flexible bodies require integration between the Attitude Control System (ACS) and the structure to avoid elastic instabilities. To address the challenge of integrated spacecraft design (also called co-design), methods which tie together spacecraft structural dynamics, control laws and propulsion design methods are needed.

Integrated design relevance has increased for the last three decades due to many reasons. Firstly, it reduces prototyping time and, as a consequence, decreases development costs. Secondly, integrated design approaches allow to optimize simultaneously control laws with other subsystems, using the full design freedom of the plant to improve the closed-loop performance. For instance, structural strength and stiffness requirements could be softened if the controller which reduces the dynamical response is optimized simultaneously to compensate strength reduction, leading to many useful advantages such as mass saving, length augmentation or the minimization of the energy consumed by the located actuators. Finally, integrated design methods offer a different view from the one provided by the current design methods, where control designers have little inputs about the evolution of other subsystems. Integrated design methods can overcome these barriers and achieve a full knowledge of how some subsystem parameters affect their own requirements and other subsystems specifications.

Due to the importance of an integrated control/subsystems design methodology, many attempts have been made, mainly in structural control literature, since the publication of the first integrated design methodologies such as those in Onoda and Haftka (1987), Gilbert (1988) or Messac and Malek (1992). These methods were based on iterative methodologies with optimization algorithms. Lately, other methods have been proposed such as those solved by LMI algorithms or with LQG methods like in Hiramoto et al. (2009) and Cimellaro et al. (2008) respectively. However, these approaches give conservative results and their applicability is restricted by problem dimension.

Recently, a counterpart technique currently under development in ONERA Toulouse Research Center allows a more general approach (Alazard et al., 2013). Actually, this method is based on structured H_∞ synthesis algorithms developed in Gahinet and Apkarian (2011), granting structured controllers and tunable parameters optimization. In addition, particular properties can be imposed to the controller as well, as its internal stability or frequency template. This synthesis, merged with a correct plant modelling, can reveal important applications of integrated design methodologies.

As stated before, a correct plant modeling is needed in order to implement integrated design. Particularly for this study, the problem lies on finding a consistent plant modeling for a spacecraft considered as *flexible*. For this kind of methodology, models have to be implemented as Linear Fractional Representations (LFT) so that the tools used for structured H_∞ synthesis can be applied. In the case of this study, flexible spacecraft integrated design, a linear model which includes appendages flexible modes is needed. LTI representation methods for appendages attached to spacecraft hub have been presented with very interesting concepts in Alazard et al. (2008) and Alazard et al. (2015), based on the methods explained in Imbert and Mamode (1978) and Imbert (1979). In those studies the spacecraft is modelled as a main rigid body with one or several flexible appendages, each rigidly connected to the main body (star structure). However, they do not offer the possibility of interconnecting several flexible appendages between them. The Interconnected Flexible Appendage (IFA) model, proposed in Perez et al. (2015), has been developed to meet such purposes: appendage LFT representation which allows to interconnect several appendages in open-chain assembly, granting its usage for ACS control law synthesis.

This work aims at demonstrating Interconnected Flexible Appendage (IFA) accuracy and suitability for future usage in integrated ACS/Structure design applications which involve large chains of flexible bodies. The model is validated in the real-case application of a deployable boom from the TARANIS [1] microsatellite. To accomplish this task, first an explanation of the integrated design methodology is given. Next, a description of the modeling procedure for the deployable boom is given. Then, model dynamics are tested in a real-case scenario of an attitude maneuver. Finally, perspectives are extracted for future works in integrated design.

2. MODELS FOR INTEGRATED DESIGN BASED ON STRUCTURED H_∞ SYNTHESIS

A thorough explanation of structured H_∞ controller synthesis is given in Gahinet and Apkarian (2011). This study shows how it is possible to impose controller order, structure and stability thanks to the structured H_∞ synthesis. Figure 1 shows standard problem is composed of two elements: a Linear Fractional Representation (LFT) of the controlled system, $P(s)$, and a structured controller with tunable parameters $C(s) = diag(K_1(s), \dots, K_N(s))$.

Given $\gamma_{obj} > 0$, structured H_∞ synthesis consists on tuning the free parameters of $C(s)$ to enforce closed-loop internal stability such that:

$$||\mathcal{F}_l(P(s), C(s))||_\infty < \gamma_{obj} \quad (1)$$

and satisfy a set of design requirements in the form of M normalized H_∞ constraints, $H_1(s), H_2(s), \dots H_M(s)$, such that $||H_j(s)||_\infty < 1$ (Gahinet and Apkarian, 2011). Observing that each H_∞ requirement has the form $H_j(s) = \mathcal{F}_l(P_j(s), C(s))$, the problem can be reformulated with the controller $C(s)$ repeated multiple times in the Standard Form $P(s)$, which is a rearrangement of the input/output channels of $diag(P_1(s), \dots P_M(s))$. This is what is called the *Multi-Model H_∞ synthesis*, and it allows to impose the controller different properties besides its structure, such as its internal stability (Alazard et al., 2013), frequency template (Loquen et al., 2012) or maximum gain values.

[1] Tool for the Analysis of RAdiation from lightNing and Sprites

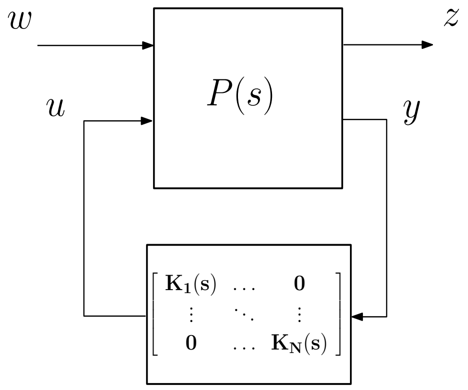

Figure 1. Standard form for structured H_∞ synthesis.

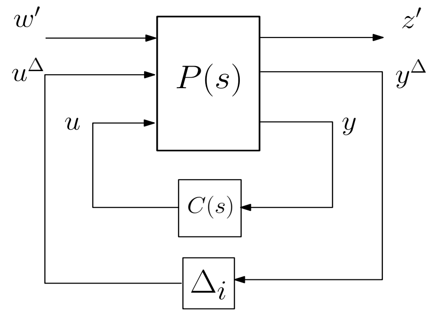

Figure 2. Integrated Design H_∞ standard form.

The *multi-model* methodology can be enlarged to include integrated design between certain tunable parameters of the controlled system $P(s)$ and the stabilizing structured controller $C(s)$, as demonstrated in (Alazard et al., 2013). This obliges to establish how the dynamical behaviour of $P(s)$ is affected by changes in those parameters. This can be included considering a LFT $P(s) - \Delta_i$, where Δ_i is the uncertainty matrix commonly used in μ-analysis. However, for integrated design case, Δ_i matrix is no longer considered as plant uncertain dynamics but as a matrix which includes how parameter variations of $P(s)$ affect its dynamical behaviour. The goal is to optimize such variations simultaneously with the controller in order to meet the normalized H_∞ constraints that could include, for example, dynamical requirements in $P(s)$ and controller requirements of $C(s)$.

In other words, the **Structured H_∞ Integrated Design Synthesis** tunes the free parameters contained in the augmented controller $K(s) = diag(C(s), \Delta_i)$ to ensure closed loop internal stability and meet normalized H_∞ requirements (Figure 2). Obviously, the difficulty lies on how to impose the correct normalized H_∞ requirements so that successful integrated design synthesis is guaranteed.

Thus, when considering integrated structure/control design of a flexible spacecraft, a **LFT representation of the different mechanical subsystems is needed** so that parametric variations can be considered in the plant model. Next sections show how the Interconnected Flexible (IFA) model explained in (Perez et al., 2015) is formed to suit integrated design requirements.

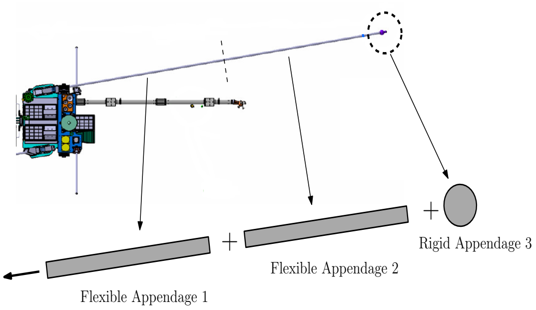

Figure 3. The deployable boom decomposition considered for IFA modelling.

3. FLEXIBLE MULTI-BODY MODELLING

As stated before, integrated structure/control design of a flexible spacecraft needs a LFT representation of the plant. However, a spacecraft is often composed of several rigid and flexible appendages attached to the main hub: solar panels, robotic arms, antennae, propellant tanks, etc. This leads to the additional problem of how to build and assemble the different LFT blocks forming the spacecraft multi-body model. An intuitive and practical breakdown for spacecraft multi-body LFT modelling has been provided in Alazard et al. (2008) for star-structure spacecraft and enlarged by Perez et al. (2015) for the case of appendages in open-chain assembly.

To illustrate the suitability of these approaches for the integrated design methodology, an example of deployable boom modelling is proposed. This boom can be considered as a multi-body open-chain composed of the following flexible and rigid appendages:

- Two flexible segments of total length $L = 4.06$ m and total mass $m_{boom} = 0.741$ Kg.
- A rigid body at the end, the Electric-Field Sensor, EFS. The EFS is approximately a sphere of $\phi = 60$ mm diameter and masse $m_{efs} = 0.085$ Kg.

The deployable boom is attached to the satellite main hub as Figure 3 shows. Segment 1 is linked to Segment 2, which is linked at its end to the rigid appendage EFS, forming an open-chain assembly of flexible-rigid bodies. The segments are thin and long, which likely implies low-frequency flexible modes that may interact with spacecraft dynamics.

The first step is to establish the LFT model of each body forming the deployable boom. In this study the flexible segments are represented with the Interconnected Flexible Appendage (IFA) approach explained in Perez et al. (2015), and the rigid appendage model is calculated as a special IFA model case. Then, concatenation must be done in order to obtain the assembled deployable model LFT representation. Parametric variations can be taken into account with the help of the IFA model, demonstrating its suitability for future integrated ACS/Structure design applications.

3.1 Flexible Appendage Model of Boom Segments

The model considered for flexible segments modelling is the IFA model. This representation allows to establish the

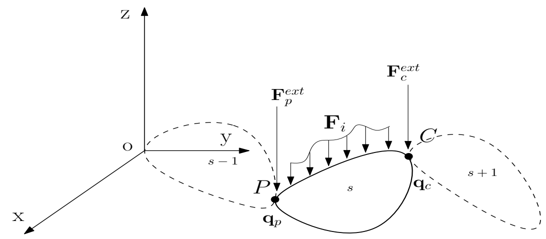

(a) Illustration of IFA model. Index s stands for the substructure or appendage being analyzed, while $s-1$ calls for the preceding appendage and $s+1$ for the next appendage in the chain.

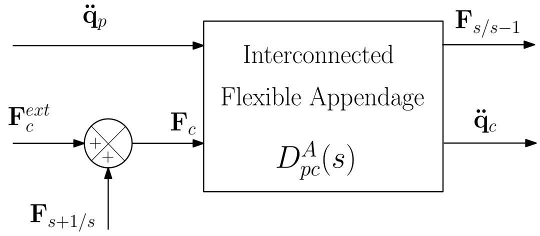

(b) Diagram Block of a nominal IFA model, $D^A_{pc}(s)$, with the respective inputs/ outputs needed for correct interconnection with other bodies (Perez et al., 2015).

Figure 4. IFA model illustration (a) and block diagram (b).

accelerations-loads transfer between the appendage connection points simultaneously with internal deformations. For this model two connection points are supposed for each appendage: one connection named P, which links with the previous appendage in the chain, and other connection named C, which links with the next appendage in the chain, as illustrated in Figure 4a.

The IFA model block diagram is depicted in Figure 4b. This representation allows to establish a cause-effect interaction between a studied appendage, noted s, and the neighbouring substructures ($s-1$ and $s+1$) through the two connection points, P and C. The flexible appendage perceives acceleration at connection point P, denoted by $\ddot{\mathbf{q}}_p$, and the loads transmitted by the successive appendage through connection point C, denoted by $\mathbf{F}_{s+1/s}$. In exchange, it provides the acceleration at connection point C, $\ddot{\mathbf{q}}_c$, and the load transmitted to the preceding appendage through P, $\mathbf{F}_{s/s-1}$. Note that each input and output are 6 component signals for a 3D case (6 degrees of freedom).

According to Perez et al. (2015), the set of state-space representations to build the IFA model are:

$$\begin{cases} \begin{bmatrix} \dot{\zeta}_l \\ \ddot{\zeta}_l \end{bmatrix} = \mathbf{A}_{IDM} \begin{bmatrix} \zeta_l \\ \dot{\zeta}_l \end{bmatrix} + \mathbf{B}_{IDM} \begin{bmatrix} \ddot{\mathbf{q}}_p \\ \mathbf{F}_c \\ \ddot{\eta}_k \end{bmatrix} \\ \begin{bmatrix} \ddot{\mathbf{q}}_c \\ \mathbf{F}_{s/s-1} \end{bmatrix} = \mathbf{C}_{IDM} \begin{bmatrix} \zeta_l \\ \dot{\zeta}_l \end{bmatrix} + \mathbf{D}_{IDM} \begin{bmatrix} \ddot{\mathbf{q}}_p \\ \mathbf{F}_c \\ \ddot{\eta}_k \end{bmatrix} \end{cases} \tag{2}$$

$$\begin{cases} \begin{bmatrix} \dot{\boldsymbol{\eta}}_k \\ \ddot{\boldsymbol{\eta}}_k \end{bmatrix} = \begin{bmatrix} \mathbf{0} & \mathbf{I} \\ -\mathbf{k}_k & \mathbf{0} \end{bmatrix} \begin{bmatrix} \boldsymbol{\eta}_k \\ \dot{\boldsymbol{\eta}}_k \end{bmatrix} + \begin{bmatrix} \mathbf{0} & \mathbf{0} \\ -\bar{\mathbf{M}}_{pk}^T & -\bar{\mathbf{M}}_{ck}^T \end{bmatrix} \begin{bmatrix} \ddot{\mathbf{q}}_p \\ \ddot{\mathbf{q}}_c \end{bmatrix} \\ \ddot{\eta}_k = [-\mathbf{k}_k \;\; \mathbf{0}] \begin{bmatrix} \boldsymbol{\eta}_k \\ \dot{\boldsymbol{\eta}}_k \end{bmatrix} + [-\bar{\mathbf{M}}_{pk}^T \;\; -\bar{\mathbf{M}}_{ck}^T] \begin{bmatrix} \ddot{\mathbf{q}}_p \\ \ddot{\mathbf{q}}_c \end{bmatrix} \end{cases} \tag{3}$$

Table 1. 3D beam properties for boom flexible segments modeling.

Material Properties	Segment 1	Segment 2
Young Modulus E	71 GPa	71 GPa
Shear Modulus G	26.7 GPa	26.7 GPa
Average Density ρ_f	1600 Kg/m^3	1600 Kg/m^3
Cross-Inertia Section I_f	535.230 mm^4	535.230 mm^4
Length L	2.030 m	2.030 m

where $\mathbf{A}_{IDM}$, $\mathbf{B}_{IDM}$, $\mathbf{C}_{IDM}$ and $\mathbf{D}_{IDM}$ are matrices of suitable size, obtained with the method used in Perez et al. (2015). State-Space (2) is the Interface Dynamic Model (IDM) and is looped with state-space (2) which is the interior dynamics model. The sub-matrices $\bar{\mathbf{M}}_{pk}$ and $\bar{\mathbf{M}}_{ck}$ are the modal participation matrices of the fixed-base modes at connection points P and C. The generalized stiffness matrix, $\mathbf{k}_k$, contains the natural frequencies of the fixed base modes. The set η_k is the set of modal coordinates of appendage interior displacements, and ζ_l are the modal coordinates associated to connection C flexible displacements as explained in Perez et al. (2015). As it can be appreciated, IFA model needs a certain amount of parameters obtained from Finite Element Model (FEM) analysis. These parameters correspond to the Craig-Bampton transformation (Craig and Bampton, 1968) of the obtained degrees of freedom (*dof*) of each substructure.

For this study the required FEM data has been obtained considering the flexible segments as 3D beams made of aluminum honeycomb (Table 1). Then, a simple FEM calculation of a 3D beam allows to obtain the desired parameters for each segment modeling. These parameters, after applying the method described in Perez et al. (2015), allow to obtain the state-space representation (2)- (3) for each boom segment. The validity of the models cannot be tested for the moment since comparison data is only available for the entire deployable boom. As a consequence it will be validated in Section 3.3 after appendage concatenation.

3.2 Rigid Appendage Model of EFS

The Electric Field Sensor (EFS) has been considered as a rigid body attached to the end of the terminal flexible segment. This appendage corresponds to the *terminal appendage* case explained in Perez et al. (2015). However, since the appendage is considered to be rigid, there are no flexible states inside the model, leading to the simple algebraic equation:

$$\mathbf{F}_{s/s-1} = -\bar{\mathbf{M}}_{pp}\ddot{\mathbf{q}}_p \tag{4}$$

where $\bar{\mathbf{M}}_{pp}$ corresponds to the rigid modes matrix, already used in Alazard et al. (2008) and Imbert (1979), and is written as follows:

$$\bar{\mathbf{M}}_{pp} = \begin{bmatrix} m_{efs}\mathbf{I} & m_{efs}(*\mathbf{GP}) \\ -m_{efs}(*\mathbf{GP}) & \mathbf{J}_G^s - m_{efs}(*\mathbf{GP})^2 \end{bmatrix} \tag{5}$$

where m_{efs} is the mass of the appendage (0.085 kg), $\mathbf{J}_G^s$ is the appendage inertia matrix at its gravity center, and $*\mathbf{GP}$ is the antisymmetric matrix associated to the gravity center position, G, from the connection point P, denoted by the vector $\boldsymbol{GP}$. The EFS being considered to be a sphere, computation of $\mathbf{J}_G^s$ and $*\mathbf{GP}$ is obvious.

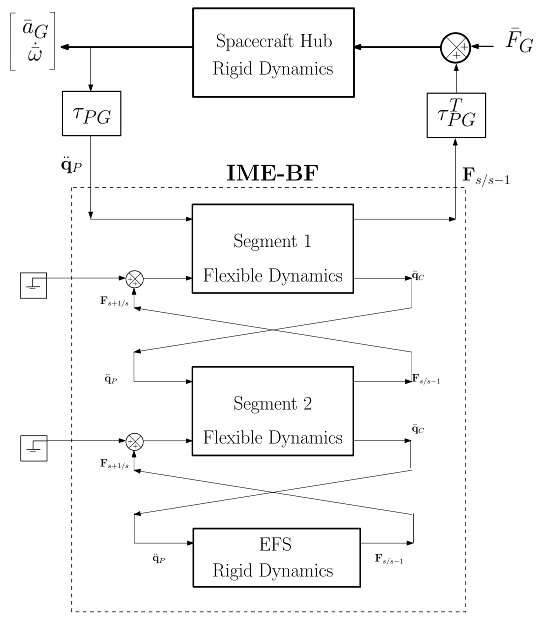

Figure 5. Deployable Boom (noted IME-BF) concatenation of segments 1, 2 and EFS.

Table 2. Results of IFA model concatenation compared with real data from TARANIS deployable boom, with and without EFS. *VBM: Vertical Bending Mode*, *LBM: Lateral Bending Mode*

Property	Real Boom Data	IFA + EFS	IFA NO EFS
Length L	4.12 m	4.12 m	4.06 m
Mass m_{boom}	0.826 Kg	0.826 Kg	0.741 Kg
1^{st} VBM	0.450 Hz	0.449 Hz	0.513 Hz
1^{st} LBM	0.4500 Hz	0.4489 Hz	0.5134 Hz

Equation (5) shows that EFS model corresponds to a constant gain which transforms the acceleration at the connection point into a load through a simple mass and inertia multiplication. Therefore, this model has one input, the acceleration of connection point P, and one output, the load transmitted to connection point at P, closing the open-chain like a feedback gain as illustrated in Figure 5.

3.3 Multi-Model Assembly and Validation Results

Once the corresponding models for each appendage in the chain are obtained, appendages are concatenated forming what is called the assembled deployable boom LTI representation. The concatenation follows the same procedure explained in Perez et al. (2015) and is illustrated in Figure 5.

After the concatenation process the full LTI representation of the deployable boom is found. Note that the interconnection can be easily done using LFT multiplication. The obtained model is compared with the real deployable boom data. Results are shown in Table 2 for different appendage concatenations (with and without EFS integration at the end).

As it can be appreciated from Table 2, the real flexible modes of the structure are accurately found using the IFA model concatenation. It is interesting to note that the introduction of a rigid body at the end (the EFS) decreases vertical and lateral bending frequencies. In Section 3.4 a deeper study of this effect is performed thanks to the variation of appendage parameters.

Therefore, the IFA modeling has demonstrated its validity since the same frequency flexible modes of the assembled structure are found. Nevertheless, loads transmitted by the appendage-chain to the main hub have to be validated as well. This aspect is evaluated later in Section 4 where the dynamical behaviour of the microsatellite TARANIS is simulated with the IFA model implementation.

3.4 Structural parameters variation for integrated design

As stated in Section 2, integrated design needs a LFT representation of the controlled plant in order to take into account parameter variations. Therefore, the last step in the modeling process of the deployable boom lies on how to include the desired parametric variations.

The IFA model representation allows to introduce parametric variations inside the models since its state-space representation provides direct access to physical parameters. For this case, EFS mass, first segment length and second segment length are considered as "uncertain" variations inside the model, leading to a LFT representation of the deployable boom depicted in Figure 6. At this stage of the study, variation in mass and length are introduced bias the $\mathbf{D}_{IDM}$ which contains in one of its blocks the $\bar{\mathbf{M}}_{pp}$ matrix. The Δ_i block size of the corresponding deployable boom block (see Figure 6) is 16×16, with 6 repetitions related to the mass variation $\Delta_{m_{efs}}$ and 5 for each length variation (Δ_{L_1} and Δ_{L_2} respectively). The effect of the these variations in the bending frequencies of the concatenated model is depicted in Figure 7, which shows that, as deducted in Section 3.3, an increase of EFS mass leads to low frequency modes, what implies a major interaction hub-appendage which affects controller optimization.

As a result, when integrated design synthesis is performed, mass and length variations in the dynamical behavior of the spacecraft are optimized to meet the desired requirements, such as minimal mass or maximal deployable length. In addition, internal system stability will be ensured.

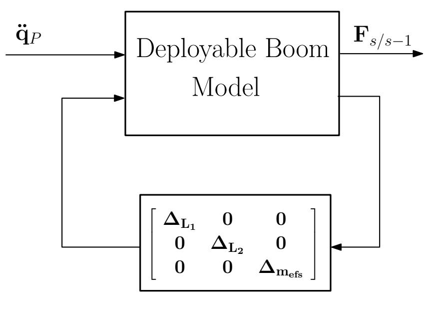

Figure 6. Complete deployable boom model taking into account variations of some parameters which form the open-chain, $\Delta_i = diag(\Delta_{L_1}, \Delta_{L_2}, \Delta_{m_{efs}})$.

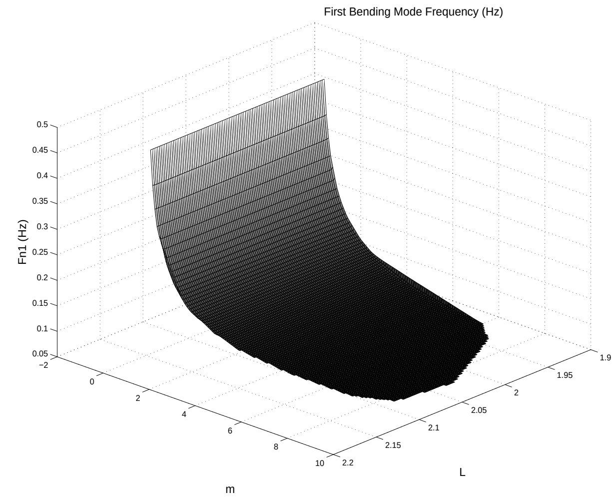

Figure 7. 3D plot showing the effect of EFS mass and first segment length variations in the first bending mode frequency (Axis x: L_1 (m); y: m_{efs} (Kg); z: 1st bending mode (Hz)).

4. MODEL DYNAMICS VALIDATION

The frequency modes of the model obtained with the IFA model of the deployable boom are the same ones as those from the real deployable boom. Nevertheless, model validation also needs to test that the Control Structure Interaction (CSI) of the obtained model approximately coincides with the real spacecraft behaviour; i.e, to test if the concatenated IFA models representing the deployable boom accurately represent flexibility perturbation in spacecraft rigid behavior. To achieve this, two simulations have been run: one implements the concatenated IFA model representing the deployable boom and the other one implements an approximation used by the French Space Agency for validation.

The simulation scenario consists in a rotation manoeuvre of angle $\theta = 30°$. The spacecraft has two kind of actuators, reaction wheels and magnetorquer, so that it can reach the given angle. The implemented control law (Proportional-Derivative) commands both actuators in order to control the maneuver. The control law has been synthesized taking into account flexibility effects with the other model. If IFA model is correct, the dynamical behavior of the spacecraft during maneuver should be close to the one obtained with the other approximation.

The same dynamical behaviour of the spacecraft is proven by the graphic shown in Figure 8. As it can be noted, angular acceleration (and by integration the angular rate) obtained with the IFA model is similar to the nominal simulation one. The error between both curves is acceptable for integrated design applications. Flexibility effects are related to the secondary angular acceleration peaks located at $t \simeq 1080$ s and $t \simeq 1250$ s. In addition, the torque needed to complete the maneuver is almost equal to the nominal simulation as well (Figure 9).

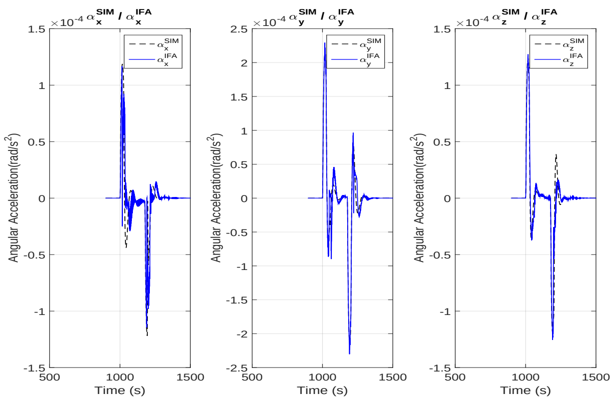

Figure 8. Angular Acceleration of TARANIS microsatellite during $\theta = 30°$ manoeuvre at $t = 1000s$. Superscript SIM stands for the nominal simulation and superscript IFA stands for the simulation with IFA model.

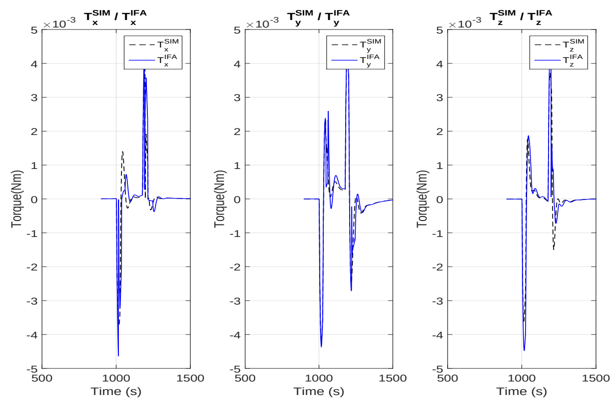

Figure 9. Torque provided by reaction wheels of TARANIS microsatellite during $\theta = 30°$ manoeuvre at $t = 1000s$. Superscript SIM stands for the nominal simulation and superscript IFA stands for the simulation with IFA model..

5. CONCLUSIONS AND PERSPECTIVES

This study has established how to drive integrated design methodology for structure/control design of spacecraft, with the simultaneous consideration of structural dynamics and control laws. This implies a correct modeling of the plant and the controller, both including design parameters so that they can be optimized simultaneously. The Interconnected Flexible Appendage (IFA) model (Perez et al., 2015) has proven its validity for this task as it conserves the same flexible modes and has the same dynamical behavior when attached to spacecraft main hub.

As for the future, structural optimization can be performed with this integrated design methodology: mass minimization, length maximization or control power minimization. Once design parameter optimization is mastered, the method can be extended to include sensor and actuator placement as an additional design objective.

All the operations for building the IFA models and connections between them are being implemented as a complement of the Matlab package *Spacecraft Dynamics Toolbox* explained in Alazard et al. (2008). As for the future, the use of IFA model in integrated design and robust control utilities is foreseen, particularly for a preliminary study for a satellite with a long chain of flexible appendages.

ACKNOWLEDGEMENTS

The authors want to thank the CNES AOCS department for providing for this study the deployable boom structural data and TARANIS dynamics simulator.

REFERENCES

Alazard, D., Cumer, C., and Tantawi, K. (2008). Linear dynamic modeling of spacecraft with various flexible appendages and on-board angular momentums. In *7th ESA Guidance, Navigation and Control Conference*. Tralee (Ireland).

Alazard, D., Loquen, T., de Plinval, H., and Cumer, C. (2013). Avionics/Control co-design for large flexible space structures. In *AIAA Guidance, Navigation, and Control (GNC) Conference*. Boston, Massachusetts, USA.

Alazard, D., Perez, J.A., Loquen, T., and Cumer, C. (2015). Two-input two-output port model for mechanical systems. In *AIAA Science and Technology Forum and Exposition*. Kissimmee , Florida. Accepted.

Cimellaro, G., Soong, T., and Reinhorn, A. (2008). Optimal integrated design of controlled structures. In *14th World Conference on Earthquake Engineering*. Beijing, China.

Craig, R. and Bampton, M. (1968). Coupling of substructures for dynamic analysis. *AIAA Journal*, 6(7).

Gahinet, P. and Apkarian, P. (2011). Structured H-infinity synthesis using MATLAB. In *18th IFAC World Congress*. Milano, Italy.

Gilbert, M.G. (1988). Results of an Integrated Structure/Control Law design sensitivity analysis. Technical Report NASA TM-101517, NASA, NASA Langley Research Center, Hampton, VA 23665-5225.

Hiramoto, K., Mohammadpour, J., and Grigoriadis, K. (2009). Integrated Design of System Parameters, Control and Sensor Actuator Placement for Symmetric Mechanical Systems. In *48th IEEE Conference on Decision and Control*. Shanghai, China.

Imbert, J. (1979). *Analyse des Structures par Elements Finis*. ENSTA. CEPAD, cepaudes edition.

Imbert, J. and Mamode, A. (1978). La masse effective, un concept important pour la caractrisation dynamique des structures avec excitation de la base. Thorie et applications. Technical Report 83, CNES.

Loquen, T., de Plinval, H., Cumer, C., and Alazard, D. (2012). Attitude control of satellite with flexible appendages: structured H-infinity approach. In *AIAA Guidance, Navigation, and Control (GNC) Conference*. Mineapolis (Minesota).

Messac, A. and Malek, K. (1992). Control Structure Integrated Design. *AIAA Journal*, 30(8), 2124–2131.

Onoda, J. and Haftka, R. (1987). An approach to structure/control simultaneous optimization for large flexible spacecraft. *AIAA*, 25, 1133–1138.

Perez, J., Alazard, D., Loquen, T., Cumer, C., and Pittet, C. (2015). Linear dynamic modelling of spacecraft with open-chain assembly of flexible bodies for AOCS/Structure Co-design. In *EURO Guidance, Navigation and Control Conference*. Submitted.